

# Multi-Rank Subspace Change-Point Detection for Monitoring Robotic Swarms

Jonghyeok Lee, Yao Xie, Youngser Park, Jason Hindes, Ira Schwartz, Carey Priebe

June 24, 2025

## Abstract

We study the problem of real-time detection of covariance structure changes in high-dimensional streaming data, motivated by applications such as robotic swarm monitoring. Building upon the spiked covariance model, we propose the *multi-rank Subspace-CUSUM* procedure, which extends the classical CUSUM framework by tracking the top principal components to approximate a likelihood ratio. We provide a theoretical analysis of the proposed method by characterizing the expected detection statistics under both pre- and post-change regimes and offer principled guidance for selecting the drift and threshold parameters to control the false alarm rate. The effectiveness of our method is demonstrated through simulations and a real-world application to robotic swarm behavior data.

## 1 Introduction

Detecting abrupt changes in high-dimensional streaming data is a fundamental problem in many modern applications, from signal processing to finance and quality control. In many applications, an important class of changes involves the covariance structure of multivariate observations. Such structural changes often reflect the emergence or switching of correlated patterns among multiple sources. For example, the onset of a critical event in a sensor array may induce a common low-dimensional signal across sensors, shifting the covariance matrix from a baseline structure of nearly identity to one with a few dominant eigenvalues. Likewise, in swarm behavior monitoring, the collective motion of agents can lie in a low-dimensional subspace, so a sudden change in behavior manifests as a low-rank change in the observation covariance. Detecting these covariance shifts rapidly and reliably is crucial for a timely response in such systems.

The *spiked covariance* model [12] provides a tractable framework for capturing low-dimensional changes in covariance. It assumes that most of the variability is concentrated in a small number of principal components, making it particularly well suited to characterizing emerging signal subspaces. In this model, the covariance matrix consists of an identity baseline plus a low-rank component capturing the dominant subspace. Prior works have developed sequential detectors for rank-1 spike changes, exploiting either the largest sample eigenvalue [24] or an estimated leading eigenvector to form CUSUM-type procedures [23]. However, real-world changes often involve multiple concurrent spikes of moderate strength, motivating a generalization to the multi-rank case. To address this, we extend the change-point detection framework by accommodating a general spiked covariance setting with an unknown multi-dimensional signal subspace.

In this paper, we propose:

- A *multi-rank Subspace-CUSUM* algorithm that tracks the top  $d$  principal directions in a rolling window and raises an alarm when their combined projection energy exceeds a threshold.
- Theoretical analyses showing how to set the drift parameter and detection threshold to achieve a prescribed average run length.
- Numerical validations on both synthetic and real-world datasets, demonstrating that the proposed method effectively detects multi-spike changes and performs robustly even when individual signals are weak.

## 1.1 Related works

Early approaches to change-point detection treated covariance shifts within the classical statistical process control. Traditional Shewhart control charts and CUSUM procedures [16] were extended to monitor covariance changes under low-dimensional settings. For instance, Hotelling’s  $T^2$  control chart [10] can detect general mean or covariance shifts, and methods based on determinants or generalized likelihood have been used to detect known covariance changes. Also, [9] studied a multivariate CUSUM procedure for a covariance shift scaled by a constant. Similarly, [8] proposed using the determinant of the sample covariance as a univariate statistic to flag a covariance change. However, these classical techniques often assumed either that the post-change covariance was fully specified or that data dimensions were modest.

More recent works have tackled covariance change detection in high-dimensional contexts with unknown change-points in an offline manner. Notably, [4] developed hypothesis tests for a change in a Gaussian covariance, using information criteria to estimate the change-point. [20] proposed a binary segmentation approach to localize multiple covariance breaks, while [3] introduced a test based on differences in inverse covariance matrices. [2] considered likelihood ratio tests for the appearance of a correlation between a specific subset of variables.

Despite these advances in offline analysis, the problem of sequentially detecting covariance structure changes in real time remains relatively underexplored. [11] studied the sequential detection of a subspace switch using a CUSUM-type procedure; however, their method requires knowing the post-change subspace in advance. Recently, [7] took a random matrix theory perspective to devise a hypothesis test for changes in the leading eigenvalues of a high-dimensional covariance sequence. [25] Our work builds most directly on [23, 24], who introduced sequential procedures for detecting when the covariance matrix shifts to a spiked model with an unknown principal component. In particular, they proposed a sliding-window largest eigenvalue chart and a subspace CUSUM detector on a single spike model.

Moreover, many methods have been developed for detecting structural changes in evolving networks. [25] proposed a spectral-CUSUM method to monitor changes in community structure by inspecting the eigen-decomposition of graph-related matrices. [18] introduced a technique to flag shifts in the large-scale connectivity pattern of an evolving network, and [22] proposed a multi-step algorithm for detection in dynamic social networks. [13] developed a sequential approach based on a spectral CUSUM statistic for detecting the emergence of communities in networks. [19] designed a data-driven Siamese graph neural network, enabling online detection of distributional changes in a network without prior model knowledge. [21] proposed an online tensor-based detection algorithm to identify changes in the latent connectivity structure across layers. Notably, [6] introduced a spectral iso-mirror embedding to reduce a dynamic network series to a scalar representation, and [5] demonstrated that a spectral Euclidean mirror technique can effectively localize “first-order” change-points in network evolution.

## 2 Problem setup

In this section, we formalize two closely related formulations. In the *emerging subspace* setting, the data arrive as pure noise until an unknown time  $\tau$  when a low-dimensional spike is added to the covariance. In the *switching subspace* problem, the nominal spike shifts to an unknown direction at time  $\tau$ . Both problems are naturally modeled by a spiked covariance model [12].

In the *emerging subspace* formulation, the observations follow a Gaussian distribution with identity covariance prior to the change, and a spiked covariance structure after the change:

$$\begin{aligned} x_t &\stackrel{\text{i.i.d.}}{\sim} N(0, \sigma^2 I_k), \quad t = 1, \dots, \tau, \\ x_t &\stackrel{\text{i.i.d.}}{\sim} N(0, \sigma^2 I_k + U \Lambda U^\top), \quad t = \tau + 1, \tau + 2, \dots, \end{aligned} \quad (1)$$

where  $\tau$  is the unknown change-point. The matrix  $U \in \mathbb{R}^{k \times d}$  contains  $d$  orthonormal columns representing the directions of the emerging signal subspace, and  $\Lambda = \text{diag}(\lambda_1, \dots, \lambda_d)$  is a diagonal matrix of signal strengths, with  $\lambda_1 \geq \dots \geq \lambda_d > 0$ . The scalar  $\sigma^2$  denotes the noise variance, which is considered known as it can be well-estimated by nominal data. We define the componentwise signal-to-noise ratio (SNR) as  $\rho_i = \lambda_i / \sigma^2$  for  $i = 1, \dots, d$ .

Alternatively, in the *switching subspace* model, both the pre- and post-change covariances have low-rank spikes, but with possibly different subspaces:

$$\begin{aligned} x_t &\stackrel{\text{i.i.d.}}{\sim} N(0, \sigma^2 I_k + U_1 \Lambda U_1^\top), \quad t = 1, \dots, \tau, \\ x_t &\stackrel{\text{i.i.d.}}{\sim} N(0, \sigma^2 I_k + U_2 \Lambda U_2^\top), \quad t = \tau + 1, \tau + 2, \dots, \end{aligned} \quad (2)$$

Here,  $U_1, U_2 \in \mathbb{R}^{k \times d}$  are both semi-orthogonal matrices representing the pre- and post-change signal subspaces, satisfying  $U_i^\top U_i = I_d$  for  $i = 1, 2$ . In this setting, the baseline subspace  $U_1$  is assumed to be known a priori from the nominal distribution.

It is worth noting that the switching subspace model can be reduced to the emerging subspace formulation by projecting the data onto the orthogonal complement of  $U_1$ . Specifically, let  $Q \in \mathbb{R}^{(k-d) \times k}$  be any semi-orthogonal matrix satisfying  $QU_1 = 0$  and  $QQ^\top = I_{k-d}$ . Define the projected observations as

$$y_t = Qx_t \in \mathbb{R}^{k-d}, \quad t = 1, 2, \dots$$

Then the sequence  $y_t$  is a random vector with distribution  $N(0, \sigma^2 I_{k-d})$  before the change, and  $N(0, \sigma^2 I_{k-d} + QU_2 \Lambda U_2^\top Q^\top)$  after the change. Denoting

$$U = QU_2 / \|QU_2\|_F, \quad \tilde{\Lambda} = \Lambda \|QU_2\|_F^2 = (d - \|U_2^\top U_1\|_F^2) \Lambda,$$

we recover an emerging subspace model of the form (1) for the projected observations as follows:

$$\begin{aligned} y_t &\stackrel{\text{i.i.d.}}{\sim} N(0, \sigma^2 I_{k-d}), \quad t = 1, \dots, \tau, \\ y_t &\stackrel{\text{i.i.d.}}{\sim} N(0, \sigma^2 I_{k-d} + U \tilde{\Lambda} U^\top), \quad t = \tau + 1, \tau + 2, \dots. \end{aligned} \quad (3)$$

Thus, the switching subspace problem can be treated within the same analytical framework as the emerging subspace case. We note that this reduction involves a loss of information due to projection onto a lower-dimensional subspace. Nonetheless, it enables the use of a unified, computationally efficient detection strategy that applies to both emerging and switching subspace scenarios.

Additionally, the new signal power  $\tilde{\Lambda}$  depends on the angles between the bases making up  $U_1$  and  $U_2$ . In particular, there exist angles  $0 \leq \phi_1 \leq \phi_2 \leq \dots \leq \phi_d \leq \pi/2$  such that the singular values of the  $d \times d$  matrix  $U_2^T U_1$  are  $\cos \phi_1, \cos \phi_2, \dots, \cos \phi_d$ . These  $\phi_i$  are the principal angles between the two  $d$ -dimensional subspaces. That is,

$$\tilde{\Lambda} \Lambda^{-1} = (d - \|U_2^T U_1\|_F^2) I_d = \left( d - \sum_{i=1}^d \cos^2 \phi_i \right) I_d = \left( \sum_{i=1}^d \sin^2 \phi_i \right) I_d,$$

which quantifies the portion of the new subspace  $U_2$  that lies outside the span of  $U_1$ .

### 3 Multi-rank Subspace-CUSUM

#### 3.1 Exact CUSUM

The CUSUM test [16] uses the log-likelihood ratio between the post-change and pre-change densities. The CUSUM statistic is defined as the maximum of the accumulated log-likelihood ratio over all possible change-point locations up to time  $t$ :

$$S_t = \max_{1 \leq j \leq t} \sum_{i=j}^t \log \frac{f_0(x_i)}{f_\infty(x_i)},$$

where  $f_\infty(\cdot)$  and  $f_0(\cdot)$  denote the probability density functions of an observation before and after the change, respectively. Equivalently,  $S_t$  can be computed recursively as [15]

$$S_t = (S_{t-1})^+ + \log \frac{f_0(x_t)}{f_\infty(x_t)}, \quad S_0 = 0,$$

where  $x^+ = \max\{0, x\}$ . That is, at each time we add the new log-likelihood ratio and reset to zero if the sum becomes negative. The stopping time for the CUSUM procedure is the first time  $t$  that  $S_t$  exceeds a preset threshold  $b$  chosen to control the false alarm rate:

$$T_C = \inf\{t > 0 : S_t \geq b\}.$$

Using the Woodbury matrix identity and properties of determinants, the instantaneous log-likelihood ratio for a new observation  $x_t$  is obtained as

$$\begin{aligned} \log \frac{f_0(x_t)}{f_\infty(x_t)} &= \log \left[ \frac{[(2\pi)^k |\sigma^2 I_k + U \Lambda U^T|]^{-1/2} \exp \left\{ -\frac{1}{2} x_t^T (\sigma^2 I_k + U \Lambda U^T)^{-1} x_t \right\}}{[(2\pi)^k \sigma^{2k}]^{-1/2} \exp \left\{ -\frac{1}{2\sigma^2} x_t^T x_t \right\}} \right] \\ &= \frac{1}{2\sigma^2} \sum_{i=1}^d \left[ \frac{\rho_i}{1 + \rho_i} (u_i^T x_t)^2 - \sigma^2 \log(1 + \rho_i) \right], \end{aligned}$$

The Exact CUSUM test statistic can thus be implemented by updating for each new sample  $x_t$  as

$$S_t = (S_{t-1})^+ + \sum_{i=1}^d \left[ \frac{\rho_i}{1 + \rho_i} (u_i^T x_t)^2 - \sigma^2 \log(1 + \rho_i) \right], \quad (4)$$

omitting the multiplicative factor  $(2\sigma^2)^{-1} > 0$ . When  $S_t$  exceeds the threshold  $b$ , we declare that a change has been detected.

This exact CUSUM is known to be the oracle procedure [15]. Notably, the update term has negative drift before change and positive drift after change. Indeed, letting  $\mathbb{E}_\infty[\cdot]$  denote expectation under the pre-change distribution and  $\mathbb{E}_0[\cdot]$  the expectation under the post-change distribution, one can see that (by Shannon's inequality)

$$\mathbb{E}_\infty \log \left( \frac{f_0}{f_\infty} \right) = -\frac{1}{2} \sum_{i=1}^d \left[ \log(1 + \rho_i) - \frac{\rho_i}{1 + \rho_i} \right] < 0,$$

while under the post change regime,

$$\mathbb{E}_0 \log \left( \frac{f_0}{f_\infty} \right) = \frac{1}{2} \sum_{i=1}^d [\rho_i - \log(1 + \rho_i)] > 0.$$

This ensures  $S_t$  will tend to drift downwards (and stay at 0) in the absence of change, but will drift upwards after the change, as desired.

### 3.2 Multi-rank Subspace-CUSUM procedure

In practice, the exact CUSUM requires *a priori* knowledge of the post-change subspace  $U$  and signal strengths  $\lambda_i$ , which is often unavailable. A straightforward generalized likelihood ratio approach would involve continuously re-estimating these parameters and plugging them into the likelihood ratio, but doing so naively at every time  $t$  would be computationally intensive. Instead, we propose the multi-rank Subspace-CUSUM procedure, which tracks an estimated signal subspace on the fly and uses it to form a scalable detection statistic.

We maintain an estimate  $\hat{U}_t \in \mathbb{R}^{k \times d}$  of the leading  $d$ -dimensional signal subspace at time  $t$ . This can be obtained by computing the sample covariance over a recent sliding window of length  $w$  and extracting its  $d$  leading eigenvectors. In other words, at each time  $t$  we form

$$\hat{\Sigma}_t = \frac{1}{w} \sum_{i=t-w+1}^t x_i x_i^T,$$

and let  $\hat{U}_t = [\hat{u}_{1,t}, \dots, \hat{u}_{d,t}] \in \mathbb{R}^{k \times d}$  be the matrix of  $d$  principal unit norm eigenvectors  $\hat{u}_{i,t}$ ,  $i = 1, \dots, d$ , of  $\hat{\Sigma}_t$ , corresponding to its  $d$  largest eigenvalues. This  $\hat{U}_t$  serves as an approximation to the true  $U$  under the post-change regime. The window size  $w$  should be large enough to reliably learn the subspace but not so large that it fails to adapt when the covariance shifts. In the initial pre-change period,  $\hat{U}_t$  will essentially track arbitrary directions in noise, but once the covariance spikes appear,  $\hat{U}_t$  will begin to align with the true signal subspace  $U$  after on the order of  $w$  samples. Thus,  $w$  can be viewed as an estimation lag that contributes to the overall detection delay.

Given a delayed subspace estimate  $\hat{U}_{t+w}$  computed over time  $[t+1, t+w]$  (practically, this is always possible by properly delaying our data by  $w$  samples), we define a scalar increment  $Z_t$  that measures how signal-like the new observation  $x_t$  is. A natural choice is the squared norm of  $x_t$  projected onto the

estimated subspace:

$$Z_t = \|\hat{U}_{t+w}^T x_t\|^2 = \sum_{i=1}^d (\hat{u}_{i,t+w}^T x_t)^2.$$

Here,  $Z_t$  represents the energy of  $x_t$  in the top- $d$  principal directions estimated from future  $w$  data.

We define the Subspace-CUSUM statistic  $S_t^{\text{sub}}$  recursively as

$$S_t^{\text{sub}} = (S_{t-1}^{\text{sub}})^+ + Z_t - \Delta, \quad S_0^{\text{sub}} = 0.$$

The drift parameter  $\Delta$  should be set between the typical values of  $Z_t$  under the no-change and change scenarios. Formally, we require the double inequality

$$\mathbb{E}_\infty[Z_t] < \Delta < \mathbb{E}_0[Z_t],$$

so that  $S_t^{\text{sub}}$  has a negative drift before the change and a positive drift after the change. The stopping time is

$$T^{\text{sub}} = \inf\{t : S_t^{\text{sub}} \geq b\}$$

for some threshold  $b$  calibrated to achieve the desired false alarm rate.

The multi-rank Subspace-CUSUM procedure involves a trade-off between estimation accuracy and detection speed. Before the procedure can reliably raise an alarm, the subspace estimate  $\hat{U}_t$  must capture the new spike directions. This estimation window of length  $w$  contributes  $w$  samples of delay after the true change-point, during which  $\hat{U}_t$  is converging to  $U$  and  $S_t^{\text{sub}}$  may not yet be growing. Once  $\hat{U}_t$  successfully approximates  $U$ , the statistic  $S_t^{\text{sub}}$  sees increments  $Z_t - \Delta$  with a positive mean, and thereafter  $S_t^{\text{sub}}$  behaves similarly to the exact CUSUM.

## 4 Analysis

### 4.1 Drift parameter

In this section, we analyse the drift parameter  $\Delta$  of the detection statistic to the rank- $d$  spiked covariance model. Recall that in the Subspace-CUSUM procedure, at each time  $t$  the statistic is updated by adding the quantity  $Z_t - \Delta$ , with a reset to zero if the sum becomes negative. The main challenge is to characterize  $\mathbb{E}_\infty Z_t$  and  $\mathbb{E}_0 Z_t$  in order to pick an appropriate  $\Delta$ . We address this by analyzing the increment term  $Z_t$  under each regime.

Importantly, by our procedure design,  $\hat{U}_{t+w}$  is computed from a moving window that does not include the current sample  $x_t$ . This assures the independence of  $\hat{U}_{t+w}$  and  $x_t$ , which greatly simplifies the analysis. That is,

$$\mathbb{E} Z_t = \mathbb{E}[\mathbb{E}[Z_t | \hat{U}_{t+w}]] = \mathbb{E}\left[\text{tr}[\hat{U}_{t+w}^T \mathbb{E}[x_t x_t^T] \hat{U}_{t+w}]\right].$$

**Pre-change increment.** Before the change,  $x_t$  follows  $N(0, \sigma^2 I_k)$  with no signal component. Since  $\mathbb{E}[x_t x_t^T] = \sigma^2 I_k$  and  $\hat{U}_{t+w}$  is semi-orthogonal, we have exactly

$$\mathbb{E}_\infty Z_t = d\sigma^2. \tag{5}$$

Thus, under pre-change distribution, the expected increment is  $d\sigma^2$ .

**Post-change increment.** To specify the post-change increment, we invoke the Central Limit Theorem argument for the eigenvectors of the sample covariance matrix  $\hat{\Sigma}_t$ . Assuming that the population eigenvalues  $\{\lambda_i : i = 1, \dots, d\}$  are distinct, each sample eigenvector  $\hat{u}_i$  is approximately Gaussian distributed around the true eigenvector  $u_i$ , with covariance scaling as  $w^{-1}$  [17]. Based on this approximation, we derive the following expression for the post-change mean of the increment. A detailed derivation can be found in Appendix A.

**Lemma 4.1** (Post-change increment). *Assume that  $\{\lambda_i : i = 1, \dots, d\}$  are distinct. Under the post-change regime, we have the following mean values of increments: As  $w \rightarrow \infty$ ,*

$$\mathbb{E}_0[Z_t] = \sigma^2 \sum_{i=1}^d (1 + \rho_i) + \frac{\sigma^2}{w} \sum_{i=1}^d (1 + \rho_i) \left[ \frac{k-1}{\rho_i^2} + \sum_{\substack{j=1 \\ j \neq i}}^d \frac{(1 + \rho_j)^2}{(\rho_i - \rho_j)^2} \right] + o\left(\frac{1}{w}\right). \quad (6)$$

In other words, with the choice of large  $w$ , the post-change increment is about  $d$  times the noise variance plus the total signal power in the  $d$  spike components.

Combining the above results, we find that in the rank- $d$  spiked covariance model,

- Pre-change increment:  $\mathbb{E}_\infty Z_t = d\sigma^2$ .
- Post-change increment:  $\mathbb{E}_0 Z_t = d\sigma^2 + \sum_{i=1}^d \lambda_i + O(1/w)$ .

As long as at least one  $\lambda_i > 0$ , we have  $\lim_{w \rightarrow \infty} \mathbb{E}_0 Z_t > \mathbb{E}_\infty Z_t$ . Thus, there is a strictly positive gap between the post-change and pre-change means of the statistic's increment, which allows us to choose a drift  $\Delta$  in between these values.

In practice, one may not know the exact  $\lambda_i$  in advance. However, we can design  $\Delta$  based on a conservative minimum signal strength. For example, suppose it is known that each signal component has SNR at least  $\rho_{\min} = \lambda_{\min}/\sigma^2$ . Then a safe choice is to set  $\Delta$  to the midpoint between the no-signal and minimal-signal expectations:

$$\Delta = d\sigma^2 + \frac{1}{2}d\lambda_{\min} = d\sigma^2 \left(1 + \frac{1}{2}\rho_{\min}\right).$$

This choice guarantees  $\mathbb{E}_\infty Z_t = d\sigma^2 < \Delta < d\sigma^2 + d\lambda_{\min} \leq \lim_{w \rightarrow \infty} \mathbb{E}_0 Z_t$ , so if  $w$  is sufficiently larger than  $k$ , the required inequality is satisfied even in the worst-case scenario when each signal component is uniformly at the minimum strength.

*Remark 4.2.* Equation (6) shows that the leading term in the post-change expectation depends only on the noise level  $\sigma^2$ , the signal-to-noise ratios  $\rho_i$ , and the window size  $w$ . Importantly, this term is independent of the specific orientation of the signal subspace  $U$ . Therefore, to estimate  $\mathbb{E}_0[\|\hat{U}^T x_t\|^2]$  in practice, one may simulate the Gaussian samples using a randomly generated semi-orthogonal matrix  $U_0 \in \mathbb{R}^{k \times d}$  and covariance  $\sigma^2 I_k + U_0 \Lambda U_0^T$ .

## 5 Numerical experiments

### 5.1 Simulations

In this section, we evaluate the Subspace-CUSUM procedure on synthetic data. We simulate sequences of  $k$ -dimensional Gaussian observations  $x_t \sim N(0, \Sigma_t)$ , where  $\Sigma_t = I_k$  for  $t \leq \tau$  before an unknown changepoint  $\tau$  and  $\Sigma_t = \Sigma_1$  for  $t > \tau$ . We consider several spiked covariance scenarios for  $\Sigma_1$ :

Table 1: Threshold  $b$  for stopping rules corresponding to  $\text{ARL} = 5000$ , calibrated by Monte-Carlo simulation:  $\Lambda = I_d$ ,  $\rho_{\min} = 0.5$ .

$w$	20		50		100	
	$b$	ARL	$b$	ARL	$b$	ARL
$k = 5, d = 2, \sigma^2 = 1$	27.54	4953.4	25.22	5024.5	23.42	5015.2
$k = 5, d = 3, \sigma^2 = 1$	25.90	4974.8	24.56	4954.5	23.55	5005.4
$k = 10, d = 2, \sigma^2 = 1$	34.62	5036.5	30.63	4966.8	27.31	5042.6
$k = 10, d = 3, \sigma^2 = 1$	33.19	4917.0	29.23	5046.5	27.35	4996.1
$k = 20, d = 2, \sigma^2 = 1$	47.65	5038.5	40.54	4955.4	34.83	4981.2
$k = 20, d = 3, \sigma^2 = 1$	44.65	5013.6	39.24	5019.0	33.49	5046.4

- *Rank-1 spike*:  $\Sigma_1 = I_k + \lambda uu^T$ , where  $u$  is a unit-norm eigenvector. We consider both a dense spike where  $u = \frac{1}{\sqrt{k}}(1, 1, \dots, 1)^T$  and a sparse spike where  $u = e_1$ .
- *Rank- $d$  spike*:  $\Sigma_1 = I_k + U\Lambda U^T$  with a  $d$ -dimensional orthonormal subspace  $U = [u_1, \dots, u_d]$ . We consider uniform spikes  $\Lambda = \lambda I_d$  where all  $d$  signal eigenvalues are equal, and non-uniform spikes  $\Lambda = \text{diag}(\lambda_1, \dots, \lambda_d)$  with eigenvalues  $\lambda_1 > \lambda_2 > \dots > \lambda_d > 0$  of varying strength.

In our experiments, we benchmark Subspace-CUSUM against the oracle Exact CUSUM, which has full knowledge of the post-change subspace, and three practical baselines: Eigenvalue Shewhart Chart [24], Hotelling’s  $T^2$  chart [10], and GLR (Generalized Likelihood Ratio) procedure.

Table 1 demonstrates the thresholds  $b$  for the Subspace-CUSUM procedure that yield an ARL of approximately 5000 under the pre-change distribution, calibrated by Monte-Carlo simulation. We show results for several combinations of ambient dimension  $k$ , subspace rank  $d$ , and sliding window length  $w$ . In all cases, the post-change signal strength was set to  $\Lambda = I_d$  with a lower bound of componentwise SNR of  $\rho_{\min} = 0.5$ .

Figure 1 illustrates the trade-off between ARL and EDD for three online detectors under the uniform spike model with  $k = 10$ ,  $d = 2$ , and window length  $w = 50$ . Each subplot corresponds to a different noise variance of  $\sigma^2 = 2, 1, 0.5$ . Across all noise levels, the Exact CUSUM attains the smallest expected detection delay (EDD) for any prescribed average run length (ARL), corroborating its theoretical optimality. When the signal-to-noise ratio is low (high noise), Subspace-CUSUM closely tracks this oracle performance, suffering only a modest additional delay. By contrast, the Eigenvalue Shewhart chart incurs substantially larger delays under weak signals, since its one-shot decision statistic reacts slowly to small shifts. As the signal-to-noise ratio increases (low noise), the Shewhart-type chart begins to outperform Subspace-CUSUM, reflecting the well-known fact that Shewhart charts excel at detecting large, abrupt changes [14].

Table 2 reports the numerical values of the EDD for each detector when its threshold is tuned to yield an ARL of 5000 under the pre-change model. We consider three ambient dimensions  $k \in \{5, 10, 20\}$  and two subspace ranks  $d \in \{2, 3\}$ , across the same three noise variances as in Figure 1. In every configuration, the Exact CUSUM attains the smallest delay, matching its oracle status. Subspace-CUSUM delivers a delay that is only slightly larger, with the gap narrowing as the signal-to-noise ratio improves (i.e.  $\sigma^2$  decreases). The Largest-Eigenvalue Shewhart chart again shows substantially higher delays at low SNR,

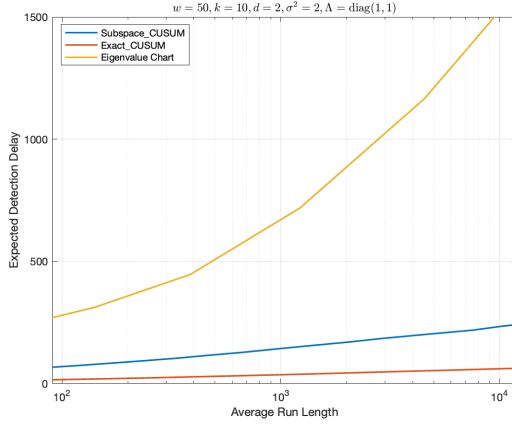
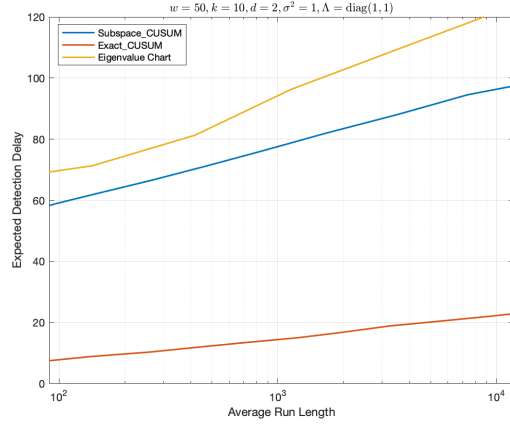
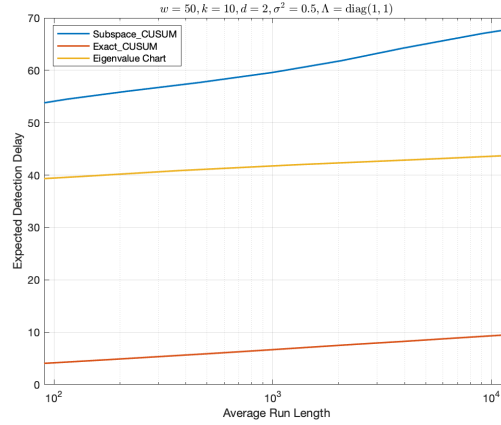
(a)  $\sigma^2 = 2$ (b)  $\sigma^2 = 1$ (c)  $\sigma^2 = 0.5$ 

Figure 1: ARL versus EDD for three detectors under varying noise levels.

though it becomes more competitive for stronger signals. These results corroborate the trade-offs between ARL and EDD seen in Figure 1 and demonstrate that Subspace-CUSUM offers a great balance between false-alarm control and rapid detection in multi-rank spiked covariance scenarios. Note that we have omitted Hotelling's  $T^2$  and the GLR procedure from Table 2, as both methods yielded enormous EDDs that closely matched the target ARL of 5000 across almost all configurations.

## 5.2 Real data

### 5.2.1 Swarm behavior data

We consider a swarm trajectory dataset consisting of  $T = 10,001$  sequential frames of collective behavior. In each frame  $t = 1, \dots, T$ , there are  $n = 100$  agents moving in a 2D plane, and we record each agent's two-dimensional positions  $P_t = \{p_{t1}, \dots, p_{tn}\}$  and velocity vectors  $V_t = \{v_{t1}, \dots, v_{tn}\}$ , where  $p_{ti}, v_{ti} \in \mathbb{R}^2, i = 1, \dots, n$ . We can construct an affinity graph, where each agent corresponds to a node,

Table 2: Simulated detection delays corresponding to ARL calibrated to 5000:  $\Lambda = I_d$ . CUSUM, S-CUSUM and EigChart stand for the Exact CUSUM, Subspace CUSUM and Eigenvalue Shewhart Chart, respectively. Hotelling’s  $T^2$  and GLR are omitted due to  $EDD \approx 5000$ .

$k$	$d$	$\sigma^2 = 2$			$\sigma^2 = 1$			$\sigma^2 = 0.5$		
		CUSUM	S-CUSUM	EigChart	CUSUM	S-CUSUM	EigChart	CUSUM	S-CUSUM	EigChart
5	2	52.9	159.6	850.2	20.1	77.1	90.6	8.4	63.7	40.1
5	3	37.9	122.3	722.8	14.4	76.2	85.8	6.0	57.8	42.9
10	2	52.5	196.3	1225.7	20.2	86.8	114.1	8.4	59.9	45.2
10	3	38.0	153.8	1043.9	15.8	75.0	100.2	6.0	62.7	50.3
20	2	52.4	349.1	2072.5	20.1	106.9	185.6	8.4	63.2	47.1
20	3	38.1	247.5	1802.0	14.4	101.2	166.4	6.0	63.2	53.7

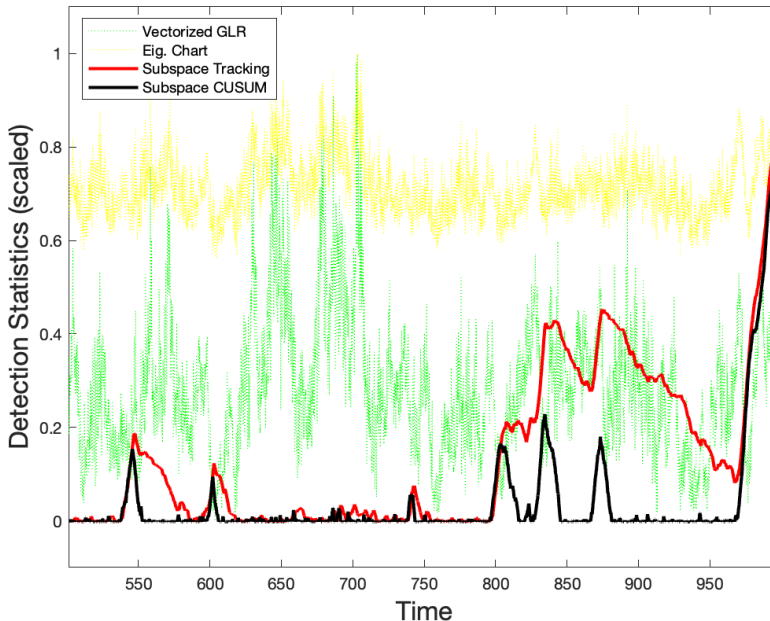


Figure 2: Detection statistics (scaled to 0-1) over time for the swarm dataset, as produced by the different change-point detection methods.

and we can observe a time series of nodal features  $\hat{X}_t = [P_t; V_t] \in \mathbb{R}^{4 \times n}$ . Let  $\tilde{X}_t$  be the position-centered and normalized nodal feature values from  $\hat{X}_t$ , which is used as the input for change-point detection.

We compare Subspace-CUSUM with three other baseline approaches, including GLR based on vectorized data, Eigenvalue Shewhart Chart, and Subspace Tracking [25]. Figure 2 illustrates the result. Subspace-CUSUM yields some clearly identifiable change points, as evidenced by a sharp rise in its detection statistic. Although no ground-truth change time is available for this real dataset, the timing of the detected change-point closely matches Subspace Tracking and an independent result obtained via the iso-mirror method of [6]. Notably, Subspace-CUSUM and [6] are founded on entirely different statistical

and algorithmic principles. The concordance between detected change-points strongly suggests that both methods are capturing the same underlying network transition.

## 6 Conclusion

We present the multi-rank Subspace-CUSUM algorithm for sequential detection of covariance structure changes in high-dimensional streams. This method extends previous subspace monitoring approaches to handle multiple concurrent spikes, offering more powerful detection capabilities in scenarios involving multiple simultaneous low-rank signals. We provide a theoretical foundation that guides the selection of key parameters to control the average run length, and we show through analysis and simulations that the proposed detector can reliably achieve the targeted performance.

Looking ahead, a key open problem is establishing the theoretical optimality of the proposed procedure. While our design is guided by asymptotic heuristics and shows strong empirical performance, a formal proof of optimality remains to be shown. Future work may also extend our framework to more general settings, such as non-Gaussian noise or time-varying covariances, and explore adaptive strategies for selecting the subspace dimension.

## Acknowledgement

This work is supported by the Office of Naval Research [N000142412278].

## References

- [1] T. W. Anderson. Asymptotic theory for principal component analysis. *The Annals of Mathematical Statistics*, 34(1):122–148, 1963.
- [2] E. ARIAS-CASTRO, S. BUBECK, and G. LUGOSI. Detection of correlations. *The Annals of Statistics*, 40(1):412–435, 2012.
- [3] V. Avanesov and N. Buzun. Change-point detection in high-dimensional covariance structure. *Electronic Journal of Statistics*, 12(2):3254 – 3294, 2018.
- [4] J. Chen and A. Gupta. Statistical inference of covariance change points in gaussian model. *Statistics*, 38(1):17–28, 2004.
- [5] T. Chen, Z. Lubberts, A. Athreya, Y. Park, and C. E. Priebe. Euclidean mirrors and first-order changepoints in network time series. *arXiv preprint arXiv:2405.11111*, 2024.
- [6] T. Chen, Y. Park, A. Saad-Eldin, Z. Lubberts, A. Athreya, B. D. Pedigo, J. T. Vogelstein, F. Pupo, G. A. Silva, A. R. Muotri, et al. Discovering a change point and piecewise linear structure in a time series of organoid networks via the iso-mirror. *Applied Network Science*, 8(1):45, 2023.
- [7] N. Dörnemann and D. Paul. Detecting spectral breaks in spiked covariance models. *arXiv preprint arXiv:2404.19176*, 2024.

- [8] J. Edward Jackson. Multivariate quality control. *Communications in Statistics-Theory and Methods*, 14(11):2657–2688, 1985.
- [9] J. D. Healy. A note on multivariate cusum procedures. *Technometrics*, 29(4):409–412, 1987.
- [10] H. Hotelling. Multivariate quality control - illustrated by the air testing of bombsights. In *Techniques of Statistical Analysis*, pages 111–184. McGraw-Hill, 1947.
- [11] Y. Jiao, Y. Chen, and Y. Gu. Subspace change-point detection: A new model and solution. *IEEE Journal of Selected Topics in Signal Processing*, 12(6):1224–1239, 2018.
- [12] I. M. Johnstone. On the distribution of the largest eigenvalue in principal components analysis. *The Annals of statistics*, 29(2):295–327, 2001.
- [13] D. Marangoni-Simonsen and Y. Xie. Sequential changepoint approach for online community detection. *IEEE Signal Processing Letters*, 22(8):1035–1039, 2014.
- [14] D. C. Montgomery. *Introduction to statistical quality control*. John Wiley & Sons, 2020.
- [15] G. V. Moustakides. Optimal stopping times for detecting changes in distributions. *the Annals of Statistics*, 14(4):1379–1387, 1986.
- [16] E. S. Page. Continuous inspection schemes. *Biometrika*, 41(1/2):100–115, 1954.
- [17] D. Paul. Asymptotics of sample eigenstructure for a large dimensional spiked covariance model. *Statistica Sinica*, pages 1617–1642, 2007.
- [18] L. Peel and A. Clauset. Detecting change points in the large-scale structure of evolving networks. In *Proceedings of the AAAI conference on artificial intelligence*, volume 29, 2015.
- [19] D. Sulem, H. Kenlay, M. Cucuringu, and X. Dong. Graph similarity learning for change-point detection in dynamic networks. *Machine Learning*, 113(1):1–44, 2024.
- [20] D. Wang, Y. Yu, and A. Rinaldo. Optimal covariance change point localization in high dimensions. *Bernoulli*, 27(1):554 – 575, 2021.
- [21] F. Wang, W. Li, O. H. M. Padilla, Y. Yu, and A. Rinaldo. Multilayer random dot product graphs: Estimation and online change point detection. *arXiv preprint arXiv:2306.15286*, 2023.
- [22] Y. Wang, A. Chakrabarti, D. Sivakoff, and S. Parthasarathy. Fast change point detection on dynamic social networks. In *Proceedings of the 26th International Joint Conference on Artificial Intelligence*, pages 2992–2998, 2017.
- [23] L. Xie, G. V. Moustakides, and Y. Xie. First-order optimal sequential subspace change-point detection. In *2018 IEEE Global Conference on Signal and Information Processing (GlobalSIP)*, pages 111–115. IEEE, 2018.
- [24] L. Xie, Y. Xie, and G. V. Moustakides. Sequential subspace change point detection. *Sequential Analysis*, 39(3):307–335, 2020.
- [25] M. Zhang, L. Xie, and Y. Xie. Spectral cusum for online network structure change detection. *IEEE Transactions on Information Theory*, 69(7):4691–4707, 2023.

## A Proofs

*Proof of Lemma 4.1.* For notational simplicity, we here denote by  $\hat{u}_i$  the  $i$ -th leading unit-norm eigenvector of the sample covariance  $\hat{\Sigma}_{t+w}$ , which is the  $i$ th column of  $\hat{U}_{t+w}$ . Under the spiked covariance model with distinct signal strengths  $\lambda_i$ , we have the following asymptotic normality of  $\hat{u}_i$  [1, 17]:

$$\sqrt{w}(\hat{u}_i - u_i) \xrightarrow{d} N(0, \Xi_i),$$

where the  $k \times k$  covariance matrix  $\Xi_i$  admits the spectral decomposition

$$\Xi_i = \sum_{\substack{j=1 \\ j \neq i}}^k \frac{\mu_i \mu_j}{(\mu_i - \mu_j)^2} u_j u_j^T, \quad \mu_j = \begin{cases} \sigma^2 + \lambda_j, & j = 1, \dots, d, \\ \sigma^2, & j = d + 1, \dots, k. \end{cases}$$

This  $\Xi_i$  can be amounted to

$$\Xi_i = \frac{1 + \rho_i}{\rho_i^2} (I_k - U U^T) + \sum_{\substack{j=1 \\ j \neq i}}^d \frac{(1 + \rho_i)(1 + \rho_j)}{(\rho_i - \rho_j)^2} u_j u_j^T.$$

Using this result, we have as  $w \rightarrow \infty$ ,

$$\begin{aligned} \mathbb{E}_0(\hat{u}_i^T x_t)^2 &= \mathbb{E}_0[\hat{u}_i^T \mathbb{E}_0[x_t x_t^T] \hat{u}_i] \\ &= \text{tr}[(\sigma^2 I_k + U \Lambda U^T) \mathbb{E}_0(\hat{u}_i \hat{u}_i^T)] \\ &= \text{tr}[(\sigma^2 I_k + U \Lambda U^T) \left( \frac{1}{w} \Xi_i + u_i u_i^T \right)] + o\left(\frac{1}{w}\right) \\ &= \sigma^2(1 + \rho_i) \left[ 1 + \frac{k-1}{w \rho_i^2} + \sum_{\substack{j=1 \\ j \neq i}}^d \frac{(1 + \rho_j)^2}{w(\rho_i - \rho_j)^2} \right] + o\left(\frac{1}{w}\right). \end{aligned}$$

Therefore, we obtain

$$\begin{aligned} \mathbb{E}_0 Z_t &= \mathbb{E}_0 \sum_{i=1}^d (\hat{u}_i^T x_t)^2 \\ &= \sigma^2 \sum_{i=1}^d (1 + \rho_i) + \frac{\sigma^2}{w} \sum_{i=1}^d (1 + \rho_i) \left[ \frac{k-1}{\rho_i^2} + \sum_{\substack{j=1 \\ j \neq i}}^d \frac{(1 + \rho_j)^2}{(\rho_i - \rho_j)^2} \right] + o\left(\frac{1}{w}\right). \end{aligned}$$

□

## B Additional experiments

### B.1 Comprehensive simulation results

We provide comprehensive simulation results for spiked covariance scenarios mentioned in Section 5.1. Tables A.1 and A.2 are results for a rank-1 spike model with a dense and sparse signal direction, respectively. Table A.3 shows the results for a multi-rank spike model with non-uniform signal strengths.

Table A.1: Rank-1 dense spike: ARL = 5000,  $\lambda = 1$ ,  $u = \frac{1}{\sqrt{k}}(1, 1, \dots, 1)^T$ .

$k$	$\sigma^2 = 2$			$\sigma^2 = 1$			$\sigma^2 = 0.5$		
	CUSUM	S-CUSUM	EigChart	CUSUM	S-CUSUM	EigChart	CUSUM	S-CUSUM	EigChart
5	90.1	211.4	550.3	35.5	97.7	136.2	14.7	65.6	57.4
10	90.6	303.2	909.7	35.1	119.1	167.1	14.7	74.3	66.4
20	90.5	644.1	2194.4	35.5	136.4	203.5	14.7	80.1	72.9

Table A.2: Rank-1 sparse spike: ARL = 5000,  $\lambda = 1$ ,  $u = e_1$ .

$k$	$\sigma^2 = 2$			$\sigma^2 = 1$			$\sigma^2 = 0.5$		
	CUSUM	S-CUSUM	EigChart	CUSUM	S-CUSUM	EigChart	CUSUM	S-CUSUM	EigChart
5	90.9	230.6	561.0	35.2	102.4	141.2	14.8	69.5	59.9
10	90.3	411.5	911.4	35.6	112.8	161.2	14.9	70.3	62.1
20	90.4	788.7	2255.1	35.4	145.8	198.4	14.8	73.0	68.7

Table A.3: Rank- $d$  non-uniform spikes: ARL = 5000,  $\Lambda = \text{Diag}(\text{linspace}(2, 1, d))$ .

$k$	$d$	$\sigma^2 = 2$			$\sigma^2 = 1$			$\sigma^2 = 0.5$		
		CUSUM	S-CUSUM	EigChart	CUSUM	S-CUSUM	EigChart	CUSUM	S-CUSUM	EigChart
5	2	28.6	90.5	324.7	11.6	63.9	67.2	5.3	56.0	38.9
5	3	20.8	76.9	256.6	8.4	61.0	63.8	3.9	54.2	35.5
10	2	28.5	109.4	581.1	11.6	65.5	76.5	5.3	56.7	43.2
10	3	20.8	90.9	403.0	8.3	59.9	71.2	3.7	54.5	40.4
20	2	28.5	153.0	1152.4	11.6	72.1	102.4	5.3	56.4	44.9
20	3	20.8	102.9	956.4	8.3	64.7	92.6	3.9	55.1	41.7